

Effect of TiO₂ Thin Film Morphology on Polyaniline/TiO₂ Solar Cell Efficiency

Amer N. J. Al-Daghman¹, K. Ibrahim¹, Naser M. Ahmed¹, Kareema M. Zaidan²

¹Nano-Optoelectronic Research and Technology Laboratory, School of Physics, University Sains Malaysia, Pulau Pinang, Malaysia

²Physics Department, Collage of Science, University of Basrah, Basrah, Iraq
Email: amer78malay@yahoo.com.my

Received 23 March 2015; accepted 18 May 2015; published 22 May 2015

Copyright © 2015 by authors and Scientific Research Publishing Inc.

This work is licensed under the Creative Commons Attribution International License (CC BY).

<http://creativecommons.org/licenses/by/4.0/>



Open Access

Abstract

Nanocrystalline titanium dioxide (TiO₂) thin films were prepared by using sol-gel through spin-coating method. An assembly of indium tin oxide (ITO)/TiO₂/polyaniline (PANI)/Ag was made in a sandwich panel structure. The obtained junction shows rectifying behavior. Additionally, the I/V characteristic indicates that a P-N junction at nanocrystalline PANI/TiO₂ interface has been created. In this experimental study, we depended only on the ratio between titanium and PANI in the process of preparing sol-gel (PANI/TiO₂ at 20% wt). The largest open circuit voltage of 656 mV and short current density of 0.00315 mA/cm² produce 0.0004% power conversion solar cell (η) under simulated solar radiation (50 mW/cm²). The thin films of PANI and titanium oxide (TiO₂)/PANI composites were synthesized by sol-gel technique. Pure TiO₂ powder with nanoparticle size of less than 25 nm and PANI were synthesized through chemical oxidative polymerization of aniline monomers. The composite films were characterized by high resolution X-ray diffraction, Fourier transform infrared spectroscopy, field effect scanning electron microscopy, and UV-vis spectroscopy. The results were compared with the corresponding data on pure PANI films. The intensity of diffraction peaks for PANI/TiO₂ composites is lower than that for TiO₂. The characteristic of the FTIR peaks of pure PANI shifts to a higher wave number in TiO₂/PANI composite, which is attributed to the interaction of TiO₂ nanoparticles with PANI molecular chains.

Keywords

TiO₂, Polyaniline, Crystal Structure, Solar Cells

1. Introduction

Photovoltaics has received increasing attention over the past decades as a feasible way to replace the diminish-

ing fossil fuels and reduce environmental damage.

Inorganic-organic heterojunction photovoltaic devices have been elicited because of their advantages, such as low cost and light weight. Inorganic semiconductor particles, such as TiO_2 [1] [2], have been used as electron acceptor in solar cells. The sol-gel method has been selected to allow the sample preparation of high-purity films at low cost. Conducting polymers used as hole transporting layers have been recently applied on photovoltaic (PV) cells. We have investigated the effect of TiO_2 nanoparticle concentration on thin film morphology and the performance of PANI/ TiO_2 solar cells.

Conducting PANI is important and has exhibited great potential for commercial applications because of its unique electrical, optical, and photoelectrical properties, as well as its easy preparation and excellent environmental stability [3] [4]. Nanocrystalline TiO_2 has also been frequently used for preparing various nanocomposites with conducting polymers because of its excellent physical and chemical properties and promising applications in advanced coatings, solar cells, gas sensors, and photo catalysts [5]. Therefore, PANI/ TiO_2 nanocomposites have been the most intensively studied among various nanocomposites, because they combine the merits of PANI and nanocrystalline titanium dioxide (TiO_2) particles within a single material and could be applied in electronic devices, nonlinear optical system, gas sensors, and photoelectrochemical devices [6] [7]. Most of the properties of these materials are based on the synergy between the properties of the components, which are a direct result of their chemical and structural compositions, and thus, can be tailored. For instance, coatings based on organic-inorganic hybrid materials have the capability to combine the flexibility and easy processing of polymers with the interesting properties of the inorganic part: hardness, thermal stability, as well as electrical and electrochemical distinguished properties. The combination of nanocrystalline titanium dioxide (TiO_2) and polyaniline (PANI) is attractive because the combination of PANI and metal oxide exhibits excellent electrical, mechanical, and optical properties, such as surface hardness, modulus, strength, transparency, high refractive index, and acids; their derivatives are highly promising coupling molecules that allow the anchoring of organic groups to inorganic solids [8] [9]. Thus, the preparation of PANI-nano- TiO_2 has been a subject of interest in many studies. Feng *et al.* synthesized a composite of PANI encapsulating TiO_2 nanoparticles through *in situ* emulsion polymerization [10].

The authors explained the nature of chain growth and interaction between PANI and nano- TiO_2 particles by Fourier transform infrared (FTIR) spectroscopic analyses [10]. Xia and Wang prepared PANI nanocrystalline titanium dioxide (TiO_2) composite through ultrasonic irradiation, which is a novel method for the preparation of 1D to 3D conducting polymer nanocrystalline composites [7]. Somani *et al.* reported the preparation of highly piezoresistive conducting PANI- TiO_2 composite through *in situ* deposition technique at low temperature (0°C) [9]. The technological relevance of both conducting PANI and semiconducting material TiO_2 in nano form leads to the preparation of a composite of PANI and TiO_2 at molecular-level interaction. Such molecular-level interaction may lead to novel properties in these two dissimilar chemical components [11]-[13]. In this paper, we report the synthesis of PANI/ TiO_2 composite by sol-gel method. Their morphological, structural, electrical, and optical properties are also studied.

2. Materials and Methods

2.1. Materials

Aniline ($\text{C}_6\text{H}_5\text{NH}$) from Merck (Schuchardt, Germany) was purified through distillation at reduced pressure before it was used. Ammonium peroxydisulfate (APS) was purchased from Merck (KGaA, Germany). Nanodimensional titanium dioxide (TiO_2 , 99.7%) and anatase nanoparticles with size <25 nm were also used.

2.2. Synthesis of Polyaniline

PANI was synthesized through the polymerization of aniline in the presence of hydrochloric acid as a catalyst and ammonium peroxydisulfate as an oxidant by chemical oxidative polymerization method. For the synthesis, 50 ml of 1 M HCl was taken, and 2 ml of aniline was added together into a 250 ml equipped with electromagnetic stirrer. Then, 5 mg of ammonium peroxydisulfate ($(\text{NH}_4)_2\text{S}_2\text{O}_8$) in 50 ml and 1 M HCl were suddenly added into the above solution. The polymerization temperature at 0°C was maintained for 5 h to complete the polymerization reaction. Then, the obtained precipitate was filtered.

The product was washed successively by 1 M HCl followed by distilled water and washed until the solution

turned colorless. Then, the product was re-filtered and thoroughly washed once again by distilled water to obtain the emeraldine salt (ES) form of PANI. To obtain the emeraldine base (EB) form of PANI, the ES form of PANI with 0.1 M NH_4OH solution was dried at 60°C in vacuum oven for 24 h. Thus, the powder of insulating PANI EB polymer was obtained [9].

2.3. Synthesis of (TiO_2/PANI) Nanocomposite

Figure 1 schematically shows that the photovoltaic device structure is ITO glass/ TiO_2 /PANI/Ag.

The device dimension for this measurement was 1 cm^2 . Titanium dioxide was used as a material for the thin films of the nanocomposite. About 4 ml of m-cresol ($\text{C}_7\text{H}_8\text{O}$) 97.7% from Acros, USA was added to the TiO_2 nanoparticle powder under vigorous stirring for 12 h for peptization. The sols were deposited on ITO conducting glass through spin-coating method at 1500 rpm for 60 s. Then, the sols were annealed at 450°C for 2 h in a tube furnace (Model: LENTON VTF/12/60/700). The TiO_2 nanoparticle with thickness of 120 was prepared through sol-gel method and annealed at 450°C and had a perfect crystalline structure. The formation of the Ti-O-Ti bonds in the films was observed after thermal treatment. However, the film became crystalline at anatase phase after annealing at 450°C .

PANI (emeraldine base, EB) powder was dissolved in 1:1 m-cresol deposit on the obtained TiO_2 thin films through spin-coating method at 3000 rpm for 60 s, and then dried at 100°C for 10 min. Afterward, the film was dried at 60°C for 24 h in an oven vacuum. Ag, an electrode, was evaporated in high vacuum with 10^{-4} Pa pressure during evaporation.

2.4. Characterization and Measurement Methods

X-ray diffraction (XRD) studies were carried out using high resolution X-ray diffractometer (Model: PANalytical X pert Pro MRD PW3040). The XRD patterns were recorded in the 2θ range of $20^\circ - 70^\circ$ with step width of 0.02° and step time of 1.25 s by using $\text{CuK}\alpha$ radiation ($\lambda = 1.5406\text{ \AA}$). XRD patterns were analyzed by matching the observed peaks with the standard pattern provided by JCPDS file. FTIR spectroscopy (Model: Perkin Elmer Spectrum Gx) of TiO_2 , PANi, and PANi: TiO_2 (20%) composite was studied in the frequency range of $400 - 4000\text{ cm}^{-1}$. Morphological study of the films of PANi and PANi: TiO_2 composite was carried out using field effect scanning electron microscopy (Model: FEI Nova NanoSEM 450) operated at 20 kV. UV-vis spectra of the samples, which were dispersed in deionized water under ultrasonication, were recorded on a Shimadzu 1800 UV-vis spectrophotometer.

The I/V characteristic measured by a Keithley 2400 current-voltage source in the dark indicated that no barrier was apparent at the Ag/PANI or ITO/ TiO_2 interface.

3. Result and Discussion

Figures 2(a)-(c) show the XRD patterns of pure PANI in EB form, TiO_2 , and PANi: TiO_2 (20%) composite. The XRD pattern of PANI shows a broad peak at $2\theta = 22.68^\circ$, which corresponds to 112 planes of PANI [10]. In **Figure 2(b)** and **Figure 2(c)**, the patterns show sharp and well-defined peaks, indicating the crystallinity of the synthesized materials. The observed 2θ values were consistent with the standard values and showed the tetragonal structure of TiO_2 [8]. **Figure 2(b)** shows that $a = 3.78\text{ \AA}$ and $c = 9.51\text{ \AA}$ [14].

The intensity of the diffraction peaks for PANi: TiO_2 composites was lower than that for TiO_2 (**Figure 2(c)**). Noncrystalline PANI reduced the volume fraction percentage of TiO_2 , and thus, weakened the diffraction peaks of TiO_2 in the composite.

| |
|-----------------------------------|
| Ag |
| PANI (196 nm)/p:type |
| TiO_2 NP (120 nm)/n:type |
| ITO conducting glass |

Figure 1. Structure of the ($1\text{ cm} \times 1\text{ cm}$) ITO glass/ TiO_2 /PANI/Ag.

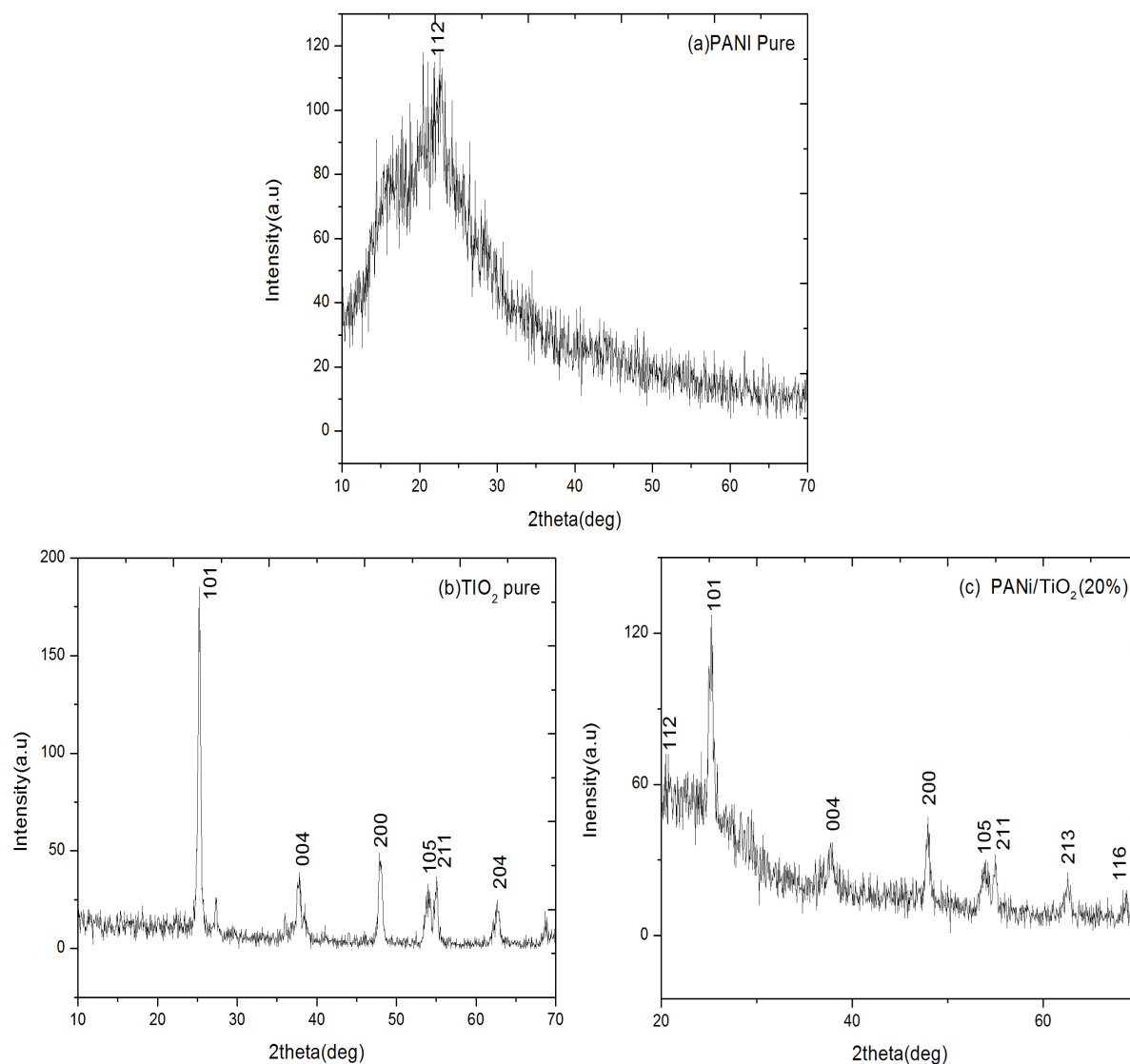


Figure 2. X-ray diffraction (a) PANi (EB), (b) TiO₂, and (c) PANi:TiO₂ nanocomposite.

Figures 3(a)-(c) show the FESEM of pure PANI, pure TiO₂, PANi:TiO₂ (20%), and nanocomposite. FESEM image of the composite shows a uniform distribution of the TiO₂ particles in the PANI chains without any agglomeration. According to the FESEM images, the nanostructure TiO₂ particles are embedded within the netlike structure built by PANI chains. The composite is highly microporous and is able to increase the liquid-solid interfacial area [15] [16].

Figures 4(a)-(c) show the FTIR spectra of the undoped PANi, PANi-TiO₂ composite, and TiO₂ nanoparticles. The origins of the vibration bands are as follows: 3365, 2922, and 622 cm⁻¹, which are caused by the NH stretching of aromatic amine, CH-stretching, and CH out-of-plane bending vibration, respectively. The CH out-of-plane bending mode has been used as a key to identify the type of substituted benzene.

The bands at 1665 and 1489 cm⁻¹ are attributed to the C=N and C=C stretching mode of vibration for the quinonoid and benzenoid units of PANI. The peaks at 1296 and 1155 cm⁻¹ are assigned to the C-N stretching mode of benzenoid ring.

The bands in the region 1000 - 1115 cm⁻¹ are caused by the in-plane bending vibration of C-H mode. The bend at 850 cm⁻¹ originates from the out-of-plane C-H bending vibration.

The low wavenumber region exhibits a strong vibration around 621 cm⁻¹, which corresponds to the antisymmetric Ti-O-Ti mode of the titanium oxide [8].

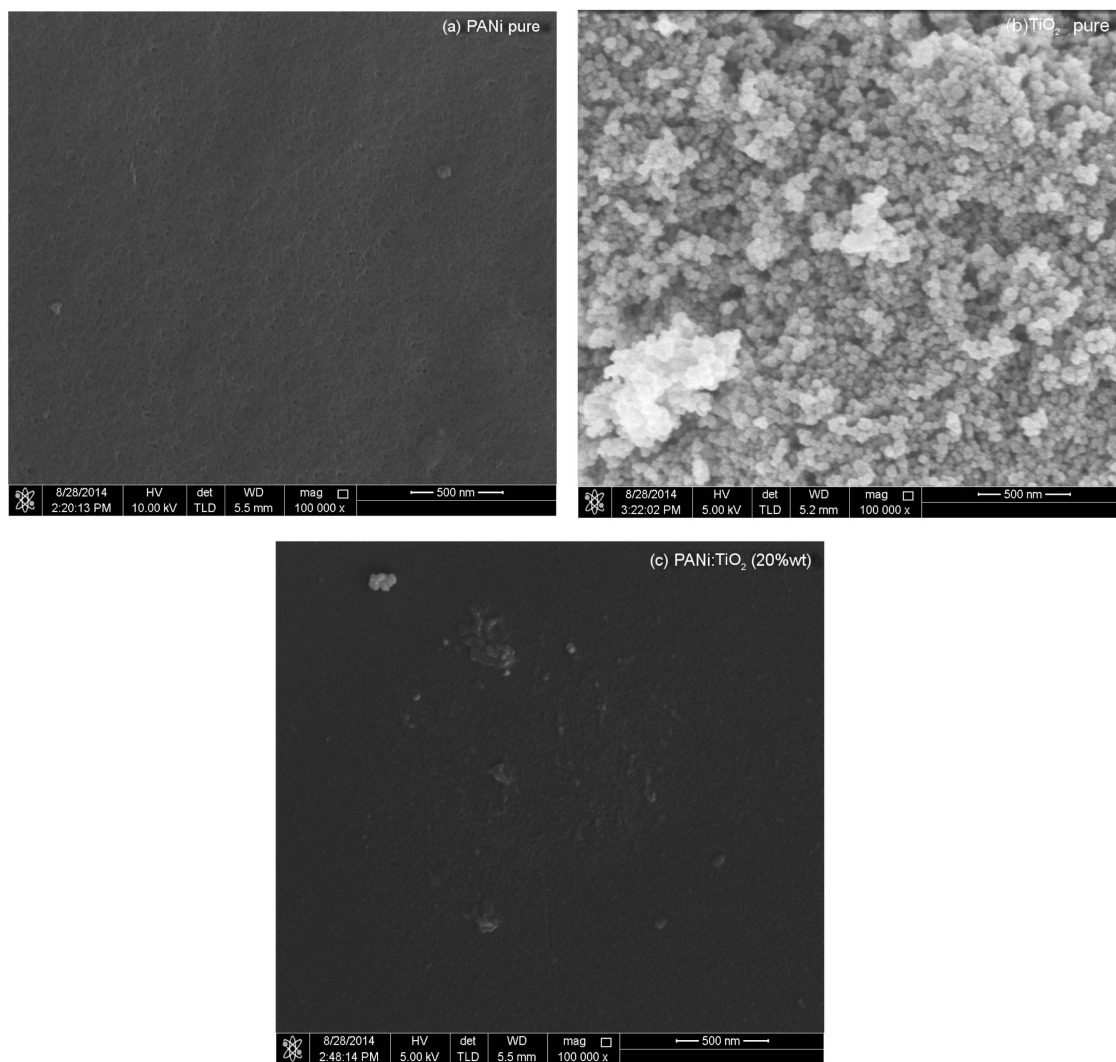


Figure 3. FESEM morphology of (a) pure PANI, (b) pure TiO₂, and (c) PANI:TiO₂ (20% wt).

The absorption of PANI pure film at the visible spectrum, which was measured on a Shimadzu UV1700 ultraviolet visible spectrophotometer, is shown in **Figure 5**.

Notably, two peaks lie at about 426 and 805 nm. These peaks indicate that the insertion of nanoparticles TiO₂ has the effect of doping the conducting PANI, and hence, should lead to an interaction at the interface of PANI and nanoparticles TiO₂. Strong terrestrial solar photon flux between 400 - 900 nm was noted. A primary factor influencing the photo-induced carrier mechanism of solar cells should also be considered. Therefore, the limiting factor of TiO₂/PANI and solar cell devices is the low absorption of photons. We could solve this issue by increasing the absorption spectrum of polyaniline in the visible zone using suitable dopants.

A built-in electric field at the nanocrystalline TiO₂/polyaniline interface has been created. **Figure 6** shows the I/V characteristics obtained from the devices under 50 mW/cm². A short-circuit current density of 3.15 mA/cm² and an open-circuit voltage of 0.656 V were obtained from device. The efficiency of the solar cell was very minimal ($\eta = 0.0004\%$) because of the increased resistance of the device, leading to the reduction of the open-circuit voltage. **Figure 6** shows the absorption spectrum of the polyaniline in the visible spectrum. The strong terrestrial solar photon flux between 400 and 900 nm should be considered a primary factor influencing the photo-induced carrier mechanism of a solar cell. This result suggests that the low absorption of photons, which is the limiting factors of TiO₂/polyaniline solar cells, might be solved by the increase of the absorption spectrum of polyaniline in the visible region by using suitable dopants.

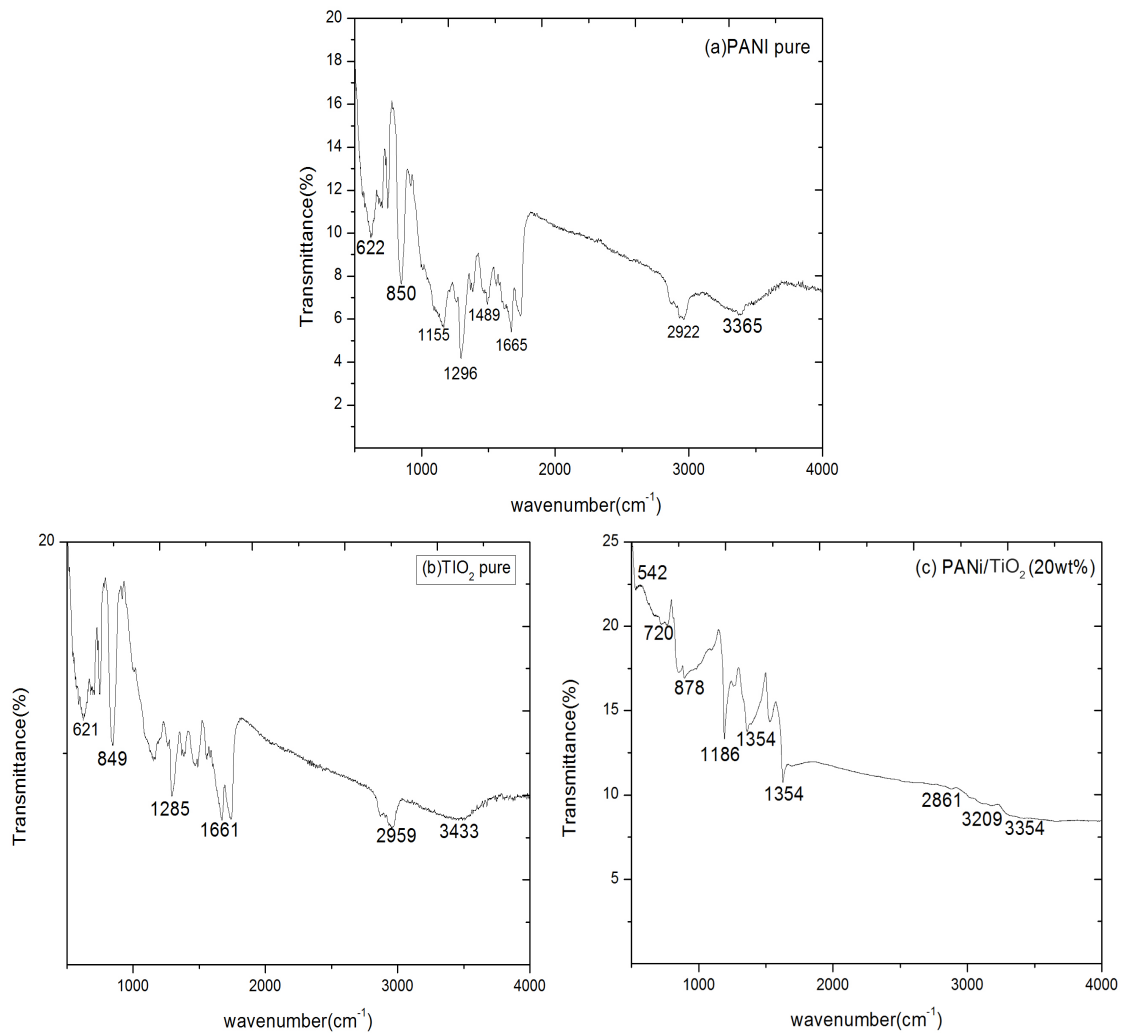


Figure 4. FTIR spectra of (a) PANI (EB), (b) PANI:TiO₂, and (c) TiO₂.

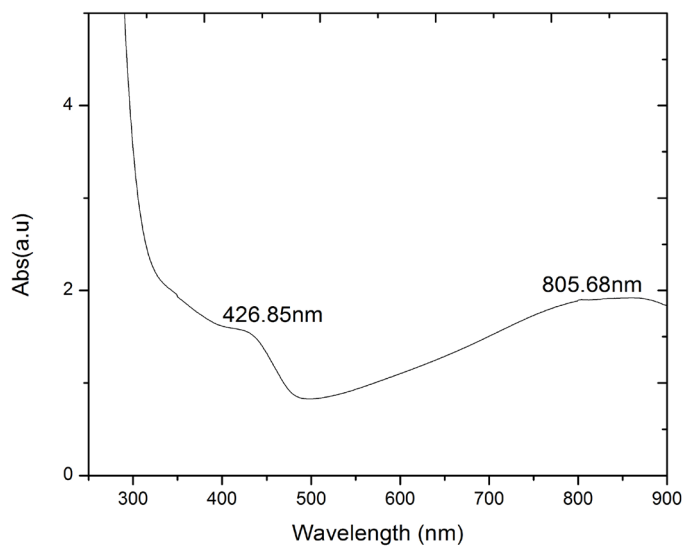


Figure 5. The absorption spectrum of polyaniline (EB) in the visible spectrum.

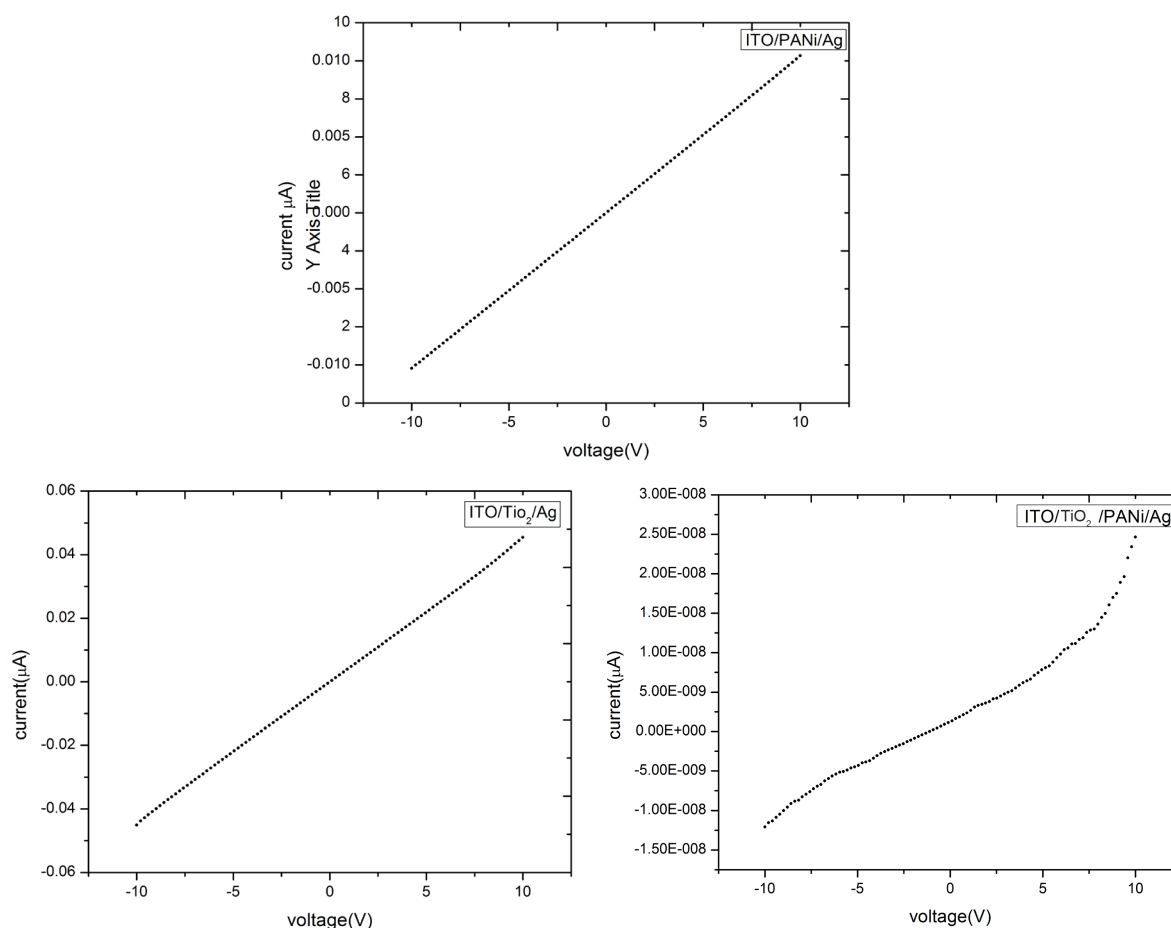


Figure 6. I/V characteristic of the sandwich-type structure of PANI, TiO₂, and ITO/TiO₂/PANI/Ag.

4. Conclusion

Thin films of conducting polymer (PANI), TiO₂ nanoparticles, and PANI/TiO₂ nanocomposites were synthesized through sol-gel method. The absorption peaks in the FTIR and UV-vis spectra of PANI/TiO₂ composite films were found to shift around higher wavenumber compared with those in pure PANI. The observed shifts were attributed to the interaction between the TiO₂ particles and polymer molecular chains PANI. A change in the value of the lattice parameter of TiO₂ in the PANI/TiO₂ composite was observed, which also indicated the presence of interaction between TiO₂ particles and PANI matrix polymer. FESEM analysis of PANI/TiO₂ composite films revealed uniform distribution of TiO₂ particles in the PANI matrix. The I/V characteristic for the device under simulated solar radiation (50 mw/cm²) has the largest open-circuit voltage of 0.656 V and short-circuit current density of 315 mA/cm².

Acknowledgements

We gratefully acknowledge the support of the School of Physics, USM, under the short-term grant nos. 203.PSF.6721001 and 304/PFIZIK/6312076.

References

- [1] Regan, B.O. and Gratzel, M. (1991) Low-Cost, High Efficiency Solar Cell Based on Dye Sensitized Colloidal TiO₂ Film. *Nature*, **353**, 737-739. <http://dx.doi.org/10.1038/353737a0>
- [2] Senadeera, G.K.R., Nakamura, K., Kitamura, T., Wada, Y. and Yanagida, S. (2003) Fabrication of Highly Efficient Polythiophene-Sensitized Metal Oxide Photovoltaic Cells. *Applied Physics Letters*, **83**, 5470-5472.

- <http://dx.doi.org/10.1063/1.1633673>
- [3] Huang, J., Virji, S., Weiller, B.H. and Kaner, R.B. (2003) Polyaniline Nanofibers: Facile Synthesis and Chemical Sensors. *Journal of the American Chemical Society*, **125**, 314-315. <http://dx.doi.org/10.1021/ja028371y>
- [4] Huang, J.X. and Kaner, R.B. (2004) A General Chemical Route to Polyaniline Nanofibers. *Journal of the American Chemical Society*, **126**, 851-855. <http://dx.doi.org/10.1021/ja0371754>
- [5] Deore, B.A., Yu, I. and Freund, M.S. (2004) A Switchable Self-Doped Polyaniline: Interconversion between Self-Doped and Non-Self-Doped Forms. *Journal of the American Chemical Society*, **126**, 52-53. <http://dx.doi.org/10.1021/ja038499v>
- [6] Tiwari, A. (2007) Gum Arabic-Graft-Polyaniline: An Electrically Active Redox Biomaterial for Sensor Applications. *Journal of Macromolecular Science, Part A*, **44**, 735-745. <http://dx.doi.org/10.1080/10601320701353116>
- [7] Roy, A.S., Anilkumar, K.R. and Ambika Prasad, M.V.N. (2011) Studies of AC Conductivity and Dielectric Relaxation Behavior of CdO-Doped Nanometric Polyaniline. *Journal of Applied Polymer Science*, **123**, 1928-1934. <http://dx.doi.org/10.1002/app.34696>
- [8] Tiwari, A., Sen, V., Dhakate, S.R., Mishra, A.P. and Singh, V. (2008) Synthesis, Characterization, and Hopping Transport Properties of HCl Doped Conducting Biopolymer-Co-Polyaniline Zwitterion Hybrids. *Polymers for Advanced Technologies*, **19**, 909-914. <http://dx.doi.org/10.1002/pat.1058>
- [9] Zhang, L.J., Wan, M.X. and Wei, Y. (2005) Polyaniline/TiO₂ Microspheres Prepared by a Template-Free Method. *Synthetic Metals*, **151**, 1-5. <http://dx.doi.org/10.1016/j.synthmet.2004.12.021>
- [10] Feng, W., Sun, E.H., Fujii, A., Wu, H.C., Niihara, K. and Yoshino, K. (2000) Synthesis and Characterization of Photoconducting Polyaniline-TiO₂ Nanocomposite. *Bulletin of the Chemical Society of Japan*, **73**, 2627-2633.
- [11] Xia, H.S. and Wang, Q. (2002) Ultrasonic Irradiation: A Novel Approach to Prepare Conductive Polyaniline/Nanocrystalline Titanium Oxide Composites. *Chemistry of Materials*, **14**, 2158-2165. <http://dx.doi.org/10.1021/cm0109591>
- [12] Somani, P.R., Marimuthu, R., Mulik, U.P., Sainkar, S.R. and Amalnerkar, D.P. (1999) High Piezoresistivity and Its Origin in Conducting Polyaniline/TiO₂ Composites. *Synthetic Metals*, **106**, 45-52. [http://dx.doi.org/10.1016/S0379-6779\(99\)00081-8](http://dx.doi.org/10.1016/S0379-6779(99)00081-8)
- [13] Matsumura, M. and Ohno, T. (1997) Concerted Transport of Electrons and Protons across Conducting Polymer Membranes. *Advanced Materials*, **9**, 357-359. <http://dx.doi.org/10.1002/adma.19970090416>
- [14] Yoneyama, H., Takahashi, N. and Kuwabata, S. (1999) Catalytic Asymmetric Reaction of Lithium Ester Enolates with Imines. *Journal of the Chemical Society, Chemical Communications*, **2**, 716-719.
- [15] Pawar, S.G., Patil, S.L., Chougule, M.A., Jundale, D.M. and Patil, V.B. (2010) Microstructural, Optical and Electrical Studies on Sol Gel Derived TiO₂ Thin Films. *Archives of Physics Research*, **1**, 57-66.
- [16] Gospodinova, N. and Terlemezyan, L. (1998) Conducting Polymers Prepared by Oxidative Polymerization: Polyaniline. *Progress in Polymer Science*, **23**, 1443-1484. [http://dx.doi.org/10.1016/S0079-6700\(98\)00008-2](http://dx.doi.org/10.1016/S0079-6700(98)00008-2)